LBL-29516
Preprint

Lawrence Berkeley Laboratory
UNIVERSITY OF CALIFORNIA

Materials & Chemical Sciences Division

Submitted to Physical Review Letters

A New Experimental Limit on the Electron Electric Dipole Moment

K. Abdullah, C. Carlberg, E.D. Commins,
H. Gould, and S.B. Ross

September 1990

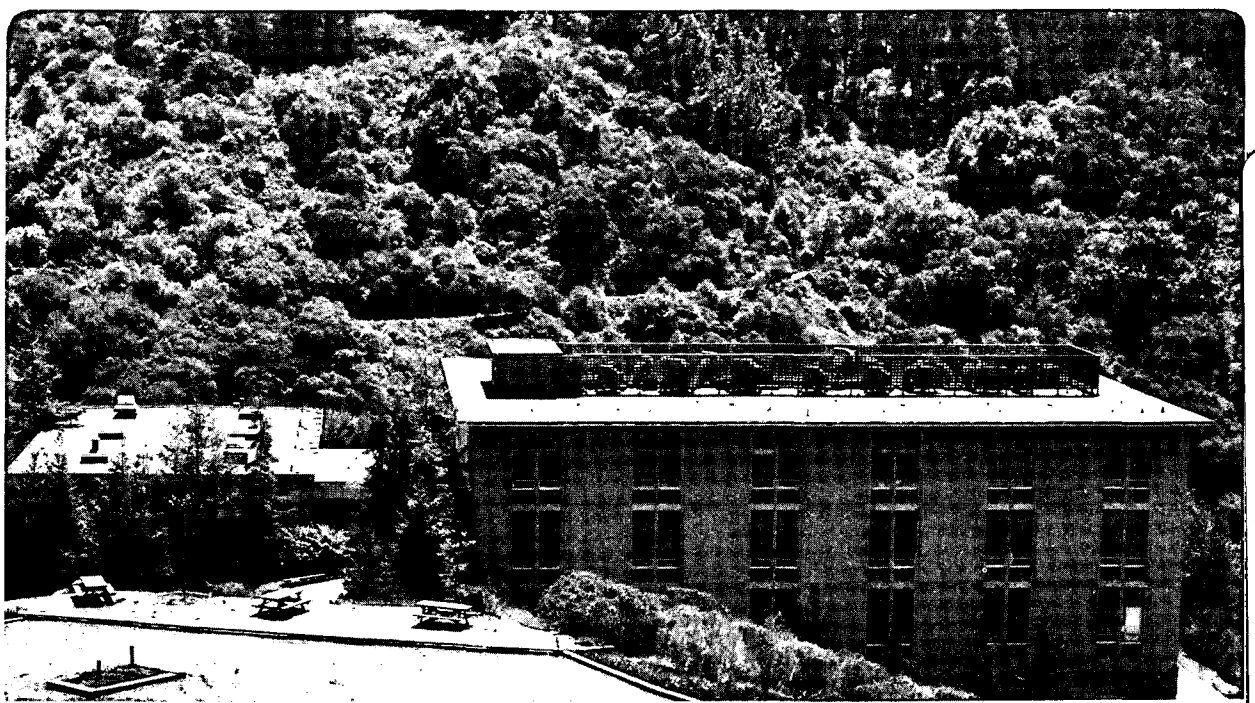

LOAN COPY
Circulates
for 2 weeks
Bldg. 50 Library.
LBL-29516
Copy 2

Prepared for the U.S. Department of Energy under Contract Number DE-AC03-76SF00098.

DISCLAIMER

This document was prepared as an account of work sponsored by the United States Government. While this document is believed to contain correct information, neither the United States Government nor any agency thereof, nor the Regents of the University of California, nor any of their employees, makes any warranty, express or implied, or assumes any legal responsibility for the accuracy, completeness, or usefulness of any information, apparatus, product, or process disclosed, or represents that its use would not infringe privately owned rights. Reference herein to any specific commercial product, process, or service by its trade name, trademark, manufacturer, or otherwise, does not necessarily constitute or imply its endorsement, recommendation, or favoring by the United States Government or any agency thereof, or the Regents of the University of California. The views and opinions of authors expressed herein do not necessarily state or reflect those of the United States Government or any agency thereof or the Regents of the University of California.

LBL-29516

A New Experimental Limit on the Electron Electric Dipole Moment

K. Abdullah[1,2], C. Carlberg[1], E. D. Commins[1,2], Harvey Gould[1], and Stephen B. Ross[1,2]

[1]Chemical Sciences Division,
Building 71-259, Lawrence Berkeley Laboratory,
One Cyclotron Road, Berkeley, CA 94720

[2]Department of Physics,
University of California, Berkeley, CA 94720

This work was supported by the U.S. Department of Energy under contract DE-AC03-76SF00098, through the Lawrence Berkeley Laboratory's Exploratory Research and Development Fund Program; and by the Director, Office of Energy Research, Office of Basic Energy Sciences, Chemical Sciences Division; and in part by the Office of High Energy and Nuclear Physics, Division of High Energy Physics and Division of Nuclear Physics.

A New Experimental Limit on the Electron Electric Dipole Moment

K. Abdullah[1,2,a], C. Carlberg[1, b], E. D. Commins[1,2], Harvey Gould[1,c], and Stephen B. Ross[1,2,d]

[1]Chemical Sciences Division,
Building 71-259, Lawrence Berkeley Laboratory,
One Cyclotron Road, Berkeley, CA 94720

[2]Department of Physics,
University of California, Berkeley, CA 94720

ABSTRACT

A search for the electron electric dipole moment d_e is carried out with two counter-propagating beams of ground state ^{205}Tl. The experiment employs atomic beam magnetic resonance with separated oscillatory fields combined with laser state selection and fluorescence detection. Extensive tests were made for possible systematic effects. The result for the atomic electric dipole moment is $d_a=(1.6 \pm 5.0)\times10^{-24}$ e cm, where the uncertainty includes equal statistical and systematic contributions. This yields $d_e=(-2.7 \pm 8.3)\times10^{-27}$ e cm, assuming the ratio $d_a/d_e = -600$.

PACS numbers 13.40.Fn, 11.30.Er 14.60.Cd, 35.10.Wb

We have made a new search for the electron electric dipole moment (EDM), which can exist only if parity (P) and time reversal invariance (T) are violated. In the standard model, where CP violation (equivalent to T violation) arises from the Kobayashi-Maskawa matrix[1], the electron EDM d_e is predicted to be no larger than 10^{-37} e cm. However, other models of CP violation predict values for d_e of experimental interest[2]; in particular, it has recently been shown that Higgs boson models[3] of CP violation can yield values of $d_e > 10^{-27}$ e cm.

The principle of our experiment is to search for d_e by measuring its energy in an electric field. While this is impractical for the free electron, it is feasible using a valence electron in a J=1/2 neutral atom of high Z, where, due to relativistic effects, the ratio R of the atomic EDM (d_a) to d_e is much larger than unity[4]. We use the 6 $^2P_{1/2}$ ground state of ^{205}Tl (Z=81) where R is estimated[5] to be -600, and search for d_a by looking for an energy splitting ΔW, linear in an applied electric field E_z, between the $m_F = \pm1$ components of the 6 $^2P_{1/2}$, F=1 state.

Systematic contributions to ΔW can arise from the interaction of the large atomic magnetic moment with any magnetic field that reverses with E_z. A motional magnetic field $\mathbf{B_{mot}} = \mathbf{E}\times\mathbf{v}/c$, where $\mathbf{v}$ is the atomic velocity, causes a splitting ΔW_{mot} that reverses with E_z if any applied magnetic field $\mathbf{B}$ is not exactly parallel to E_z. However, ΔW_{mot} reverses with $\mathbf{v}$; hence this effect is almost completely eliminated by using a pair of counter propagating atomic beams with opposite velocities.

Counter propagating beams are generated in resistively heated ovens (see Fig. 1) and propagate in vacuum with most-probable speeds $\approx 4.3\times10^4$ cm/s. We follow the up beam, which intersects a CW laser beam, directed along y and with linear polarization along z, in the state selector region. The entire experiment from here on takes place in a nominally uniform magnetic field B_z, typically 0.26 Gauss or less, in the z direction. The laser is tuned to the transition 6 $^2P_{1/2}$ (F = 1) $\rightarrow$ 7 $^2S_{1/2}$ (F = 1) at 378 nm in ^{205}Tl (See Fig. 2). Only 6 $^2P_{1/2}$ atoms with $m_F = \pm1$ make this transition because the Clebsch-Gordan coefficient, <1,0,1,0|1,0> is zero. Once excited, the atoms decay back to the 6 $^2P_{1/2}$ state, or to the 6 $^2P_{3/2}$ state with fluorescence at 535 nm, (branching ratio $\approx$ 50%). The lifetime of the latter state is long compared to the transit time of the beam through the apparatus. Hence the ground state components F = 1, $m_F = \pm1$ are depopulated and, as F = 1 atoms leave the state selector, they are in the state $m_F = 0$.

Further along the up beam trajectory is a second laser intersection region called the analyzer. (The analyzer for the up beam serves as the state selector for the down beam and vice versa.) Here, the atomic beam intersects a beam from the same laser, again directed along y with linear polarization along z, and tuned to the same transition 6 $^2P_{1/2}$, F = 1 $\rightarrow$ 7 $^2S_{1/2}$, F = 1. The analyzer fluorescence at 535 nm is our signal (S), and is proportional to the sum of the populations of F = 1, $m_F = \pm1$ atoms that enter this region. S is non-zero only if reorientation of the F = 1 state occurs in the intermediate space (because of rf and electric fields). Intersections between the laser and atomic beams in the state selector and analyzer occur at the foci of ellipsoidal mirrors with axes of revolution along z. Their purpose is to collect 535 nm fluorescence and focus it through a light pipe/optical filter system into a photomultiplier tube.

In the region between state selector and analyzer, transitions between F = 1, $m_F = 0$ and $m_F = \pm1$ are induced by oscillatory magnetic fields[6] rf1 and rf2, each 5 cm long, directed along the x axis and separated by L_{rf} =120 cm. The applied frequency $\nu = \omega/2\pi$ is set to the transition frequency $\nu_0 = \omega_0/2\pi$ to within one Hz. The transition frequency, determined by B_z, is typically 120 kHz or less. The resonance FWHM, determined by the beam transit time, is 45 Hz. Rf2 leads rf1 by a phase ϕ, which is $\pm\pi/4$ or $\pm3\pi/4$, so that $|\partial S/\partial\omega|$ is a maximum on resonance. The phase ϕ is changed every 68 ms, in order to reduce noise due to atomic and laser beam fluctuations.

In the region between rf1 and rf2 a pair of parallel titanium alloy plates of length L_E=100 cm and separation 0.2 cm is used to generate E_z, typically 110 kV/cm. The electric field is reversed every 0.93 s. Also data are taken with one beam at a time and we switch between them every 7.4 s. In order to calibrate the sensitivity to d_a, we measure the signal difference as ν is shifted by one Hz above and below ν_0 every 3.7 s. After 128 beam reversal periods have elapsed, an average EDM and its standard deviation are calculated. This result is a data point, which represents about 70 minutes of real time. Our data points are shown in Fig. 3(a,b). After each such point, all magnetic coil currents are reversed and/or the E plate cables are reversed manually, to distinguish between an EDM asymmetry and asymmetries due to systematics which are even under E and/or B.

It may be shown that near resonance, for a single beam velocity, and for optimum rf power, the analyzer signal would be proportional to:

$$S = 1 + \lambda\left[2\,\Delta\omega\frac{L_{rf}}{v} \mp \frac{\Delta W_{EDM}L_E}{\hbar\ \ v} \mp \frac{\Delta W_{syst}L_E}{\hbar\ \ v}\right] \qquad (1)$$

where $\Delta\omega = \omega - \omega_0$, the - (+) sign is employed for $B_z>0$ ($B_z<0$), $\Delta W_{EDM}=-2d_aE_z$ is the energy splitting between $m_F = \pm1$ states due to d_a, and ΔW_{syst} is the splitting arising from systematic effects. Also $\lambda=+1$ for $\phi = \pi/4$ or $-3\pi/4$, and $\lambda = -1$ for $\phi = -\pi/4$ or $3\pi/4$ for the up beam, while the sign of λ is reversed for the down beam. As is evident from (1) S contains an asymmetry proportional to the P,T odd rotational invariant $\mathbf{E}\cdot\mathbf{B}$ if $\Delta W_{EDM} \neq 0$. In reality one must take into account various features not contained in the simplified formula (1), such as the beam velocity distribution and a quadratic Stark shift between the $m_F = 0$, and $m_F = \pm1$ components.

We briefly describe important sources of systematic error (see Table 1) and steps taken to minimize them. While the $\mathbf{B}_{mot}$ systematic effect is largely eliminated by use of counter propagating beams, the following residual remains:

$$\Delta W_{mot} = \text{const} \times \{(\bar{v}_y\langle B_x/B_z\rangle - \bar{v}_x\langle B_y/B_z\rangle)_{up} + (\bar{v}_y\langle B_x/B_z\rangle - \bar{v}_x\langle B_y/B_z\rangle)_{down}\} \qquad (2)$$

where the velocities are averaged over the velocity distribution, $B_{x,y,z}$ are the magnetic field components and $\langle\ldots\rangle$ indicates an average over L_E. Let $\bar{v}_{x,y\ up} = \bar{v}_{x,y\ down} + \delta\bar{v}_{x,y}$ and $\langle B_{x,y}/B_z\rangle_{up} = \langle B_{x,y}/B_z\rangle_{down} + \delta B_{x,y}/B_z$, with $|v_x| >> |v_y|$, and $|B_z| >> |B_{x,y}|$. Inserting these expressions in (2) and dropping second order and very small terms, we obtain:

$$\Delta W_{mot} = \text{const.} \times \left(\delta\bar{v}_y\ \langle B_x/B_z\rangle - \delta\bar{v}_x\ \langle B_y/B_z\rangle + \bar{v}_x\ \delta B_y/\langle B_z\rangle\right) \qquad (3)$$

We minimize $\delta\bar{v}_y\langle B_x/B_z\rangle$ by employing auxiliary x-coils to cancel any residual B_x. The quantity $\langle B_x/B_z\rangle$ is measured by applying a known B_x and observing the change in resonance frequency on its reversal. In the second term of (3), $\delta\bar{v}_x$ is minimized by comparing the resonance widths of the up and down beams and adjusting the oven temperatures to equalize these widths to within 1%. We continuously measure $\langle B_y/B_z\rangle$ by comparing up and down beam asymmetries and maintain $\langle B_y/B_z\rangle$ at less than 1×10^{-5} on the average. The third term of (3) is non-zero if both beams do not experience the same B_y. This is possible if the two beams do not overlap exactly in y and z and if the magnetic field is inhomogeneous. Two methods are used to measure this contribution. In the first a large magnetic field gradient is imposed, we measure the EDM asymmetry and minimize it by adjusting the oven positions. In the second, the residual magnetic field inhomogeneity is determined by measuring resonant frequency shifts as we scan either atomic beam over y and z. The beam overlap is determined by measuring the difference in the resonant frequencies of up and down beams when large external magnetic field gradients are imposed. The two methods give consistent results.

A geometric phase effect arises when a magnetic field B_x exists with different values at the two ends of the electric field region x_1, x_2, and where the magnetic moment precesses many times in the lengths over which E varies between zero and its full value[7]. For $|B_z|>>|B_x|$, $|vE_z/c|$, the $m_F = \pm1$ components suffer equal and opposite phase shifts $v_xE_z(B_{x1}-B_{x2})/(cB_z^2)$, with the same sign for both beams, a result verified experimentally by deliberately imposing a large x-field gradient. If $B_{x1}-B_{x2}$ reverses when the current to the magnetic field coils reverses, the resulting asymmetry is E-odd but B-even and thus distinguishable from an EDM asymmetry. A small B-even effect is seen in our data (see below and Fig. 3). An x-field gradient that does not reverse with current may arise from leakage of external magnetic fields through our shielding. This would cause a systematic which scales with B_z^{-2}. The results of measurements made at B_z=0.085 G to set an upper limit to this effect are included in our systematic uncertainty in Table I.

Magnetic fields, synchronous with the electric field, could occur because of discharges across the electric field plates or to ground. The current flowing to the plates is monitored and E_z chosen to keep the discharge current below 10^{-8} A. We test for the effect of discharge currents by taking EDM data with larger E_z, where the discharge currents are $\approx10^{-6}$ A.

We have also calculated and/or tested for possible systematic effects due to charging currents, incomplete E reversal, phase shift errors and amplitude differences between rf1 and rf2, quadratic Stark shifts, differences in B_z at and between rf1 and rf2, different velocity distributions and backgrounds for the two beams, gravitational acceleration of the beams, calibration errors, ground loops, and insufficient delays after reversals and before restarting data collection. Among these, only contributions due to charging currents are significant at our present level of sensitivity (and are included in Table I).

Table I. Contributions to the Uncertainty in d_a (10^{-24} e cm)

Contribution	Run I B_z=0.17G	Run 2 B_z=0.255G
Exv		
Non-zero v_y and B_x	3.5	1.2
Velocity difference and residual B_y	0.3	0.3
Imperfect overlap & field gradients	3.3	0.4
Geometrical phase effect	2.4	1.0
Discharge currents	0.4	0.8
Charging currents	0.4	0.4
Total systematic uncertainty*	5.4	1.9
Statistical uncertainty	2.5	4.6

Except for infrequent automatic rejection based on excessive noise, no rejections or cuts were made nor were any corrections applied to our EDM data. There were two separate runs. Run 1, done at B_z = 0.17 Gauss, resulted in 51 data points [Fig. 3(a)]. It yielded d_a=(1.1 ± $2.5_{stat.}$ ± $5.4_{syst.}$) $\times10^{-24}$ e cm with the statistical uncertainty here as elsewhere at 68% confidence interval. The systematic uncertainty was dominated by contributions due to $\mathbf{B}_{mot}$ and geometric phase effects. In run 2 the uncertainties due to these effects were reduced, in the latter case by taking data at B_z = 0.255 G. However the noise was larger and the sensitivity to a possible EDM was decreased because we employed an electric field of 100 kV/cm, rather than 112 kV/cm, as in run 1. With 49 data points, run 2 resulted in d_a= (2.1 ± $4.6_{stat.}$ ± $1.9_{syst.}$)$\times10^{-24}$ e cm, in agreement with the result from run 1. We did a test run at B_z = 0.085 G to put a limit on the B-odd geometric phase effect and to determine the magnetic field dependence of any other systematic asymmetery. All the data taken at the three values of B_z are consistent with a B-even asymmetry proportional to B_z^{-2}. We find no evidence for any effect that is both B-odd and E-odd. We combine the statistical and systematic uncertainties in each run, and taking the resulting weighted average of the two runs we obtain: d_a=(1.6 ± 5.0)$\times10^{-24}$ e cm. Assuming R = -600, this gives d_e = (-2.7 ± 8.3)$\times10^{-27}$ e cm, where the theoretical uncertainty in R is not included. This yields a limit on d_e at least a factor of seven smaller than that obtained from all previous measurements[8,9].

We thank Alex Vaynberg for outstanding machining, Douglas McColm for his contributions to the experiment, Nelson Claytor and Narasimhan Larkin for assistance in assembling the apparatus, Alfred Wydler for assistance with electronics, and Edward Garwin, Klaus Halbach, Donald Hopkins, Iosif Khriplovich, Walter Johnson, and Mahiko Suzuki for useful discussions. This work was supported by the U.S. Department of Energy under contract DE-AC03-76SF00098, through the Lawrence Berkeley Laboratory's Exploratory Research and Development Fund Program; and by the Director, Office of Energy Research, Office of Basic Energy Sciences, Chemical Sciences Division; and in part by the Office of High Energy and Nuclear Physics, Division of High Energy Physics and Division of Nuclear Physics.

REFERENCES

(a) Present address, Salomon Brothers Inc., 1 New York Plaza, N.Y., N.Y., 10004.
(b) Present address, Manne Siegbahn Institute of Physics, Frescativ 24, 104 05, Stockholm, Sweden. Electronic mail adddress: carlberg@sesuf51.bitnet
(c) Electronic mail address: gould@lbl.bitnet
(d) Electronic mail address: stephen@ux5.lbl.gov

1. For reviews of this subject, see for example, S. M. Barr, and W. J. Marciano, in *CP violation*, C. Jarlskrog, Eds. (World Scientific, Singapore, 1989), pp. 455; and W. Bernreuther, and M. Suzuki, Lawrence Berkeley Laboratory Report LBL-27985, (1990), to be published in Rev. Mod. Phys.
2. S. M. Barr, and A. Masiero, Phys. Rev. Lett., **58**, 187 (1987).
3. S. M. Barr, and A. Zee, Phys. Rev. Lett., **65**, 21 (1990); R. G. Leigh, S. Paban, and R. M. Xu, Univ. of Texas Theory Group Report, **27-90**, (1990).
4. P. G. H. Sandars, Phys. Lett., **14**, 194 (1965).
5. P. G. H. Sandars, and R. M. Sternheimer, Phys. Rev. A, **11**, 473 (1975); V. V. Flambaum, Yad. Fiz. (Sov. J. Nucl. Phys.), **24**, 383 (1976); W. R. Johnson, D. S. Guo, M. Idrees, and J. Saperstein, Phys. Rev. A, **32**, 2093 (1985); ibid **A34**, 1043 (1986); E. Lindroth, A. M. Martensson-Pendrill, A. Ynnerman, and P. Oster, J. Phys. **B22**, 2447 (1989); A. C. Hartley, and P. G. H. Sandars, private communication (1990).
6. N. F. Ramsey, Phys. Rev., **76**, 996 (1949); Science, **248**, 1612 (1990).
7. M. V. Berry, Proc. Roy. Soc., **A392**, 45 (1984).
8. S. A. Murthy, D. Krause Jr., Z. L. Li, and L. R. Hunter, Phys. Rev. Lett., **63**, 965 (1989).
9. D. Cho, K. Sangster, and E. A. Hinds, Phys. Rev. Lett., **63**, 2559 (1989); S. K. Lamoreaux, J. P. Jacobs, B. R. Heckel, F. J. Raab, and N. Fortson, Phys. Rev. Lett., **59**, 2275 (1987); M. A. Player, and P. G. H. Sandars, J. Phys. B, **3**, 1620 (1970); H. Gould, Phys. Rev. Lett., **24**, 1091 (1970); M. C. Weisskopf, J. P. Carrico, H. Gould, E. Lipworth, and T. S. Stein, Phys. Rev. Lett., **21**, 1645 (1968).

FIGURE CAPTIONS

Fig. 1. Schematic diagram of the apparatus. The 378 nm laser beams are perpendicular to the page. Magnetic fields are produced in the z and y directions by rectangular coils, and in the x direction by circular coils. The magnetic field region is surrounded by four concentric cylindrical magnetic shields with end caps to reduce external fields. The entire apparatus is vertical as shown. If it were horizontal, gravity would affect the colinearity or velocity match of the two beams.

Fig. 2. Energy level diagram (not to scale) showing the state selection scheme.

Fig. 3. Data points for (a) Run 1, (b) Run 2, with vertical axis in units of 10^{-24} e cm. In each graph, the signs of d_a for all -B data points are reversed, for comparison with +B data points. Error bars represent standard error in the mean.

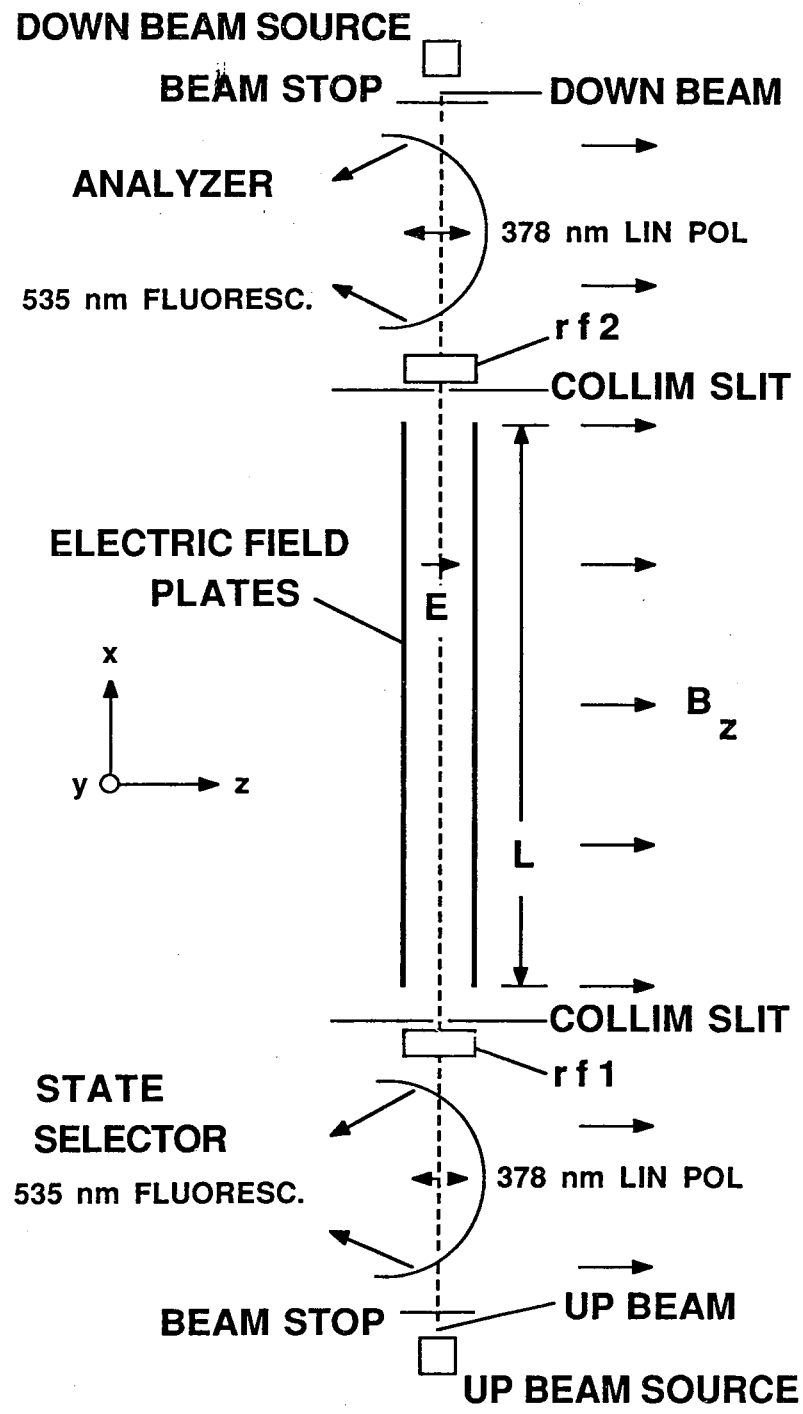

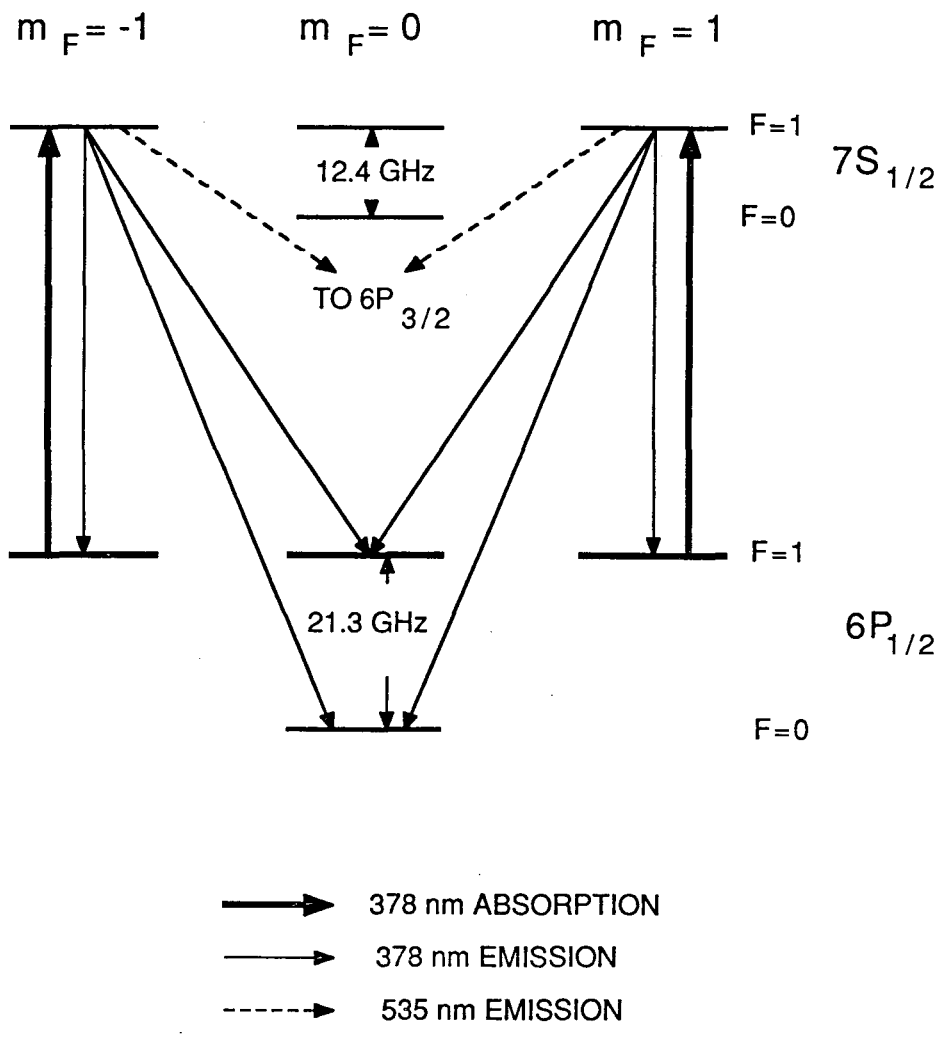
m F= -1
m F= 0
m F = 1
F=1
7S 1/2
12.4 GHz
F=0
TO 6P 3/2
F=1
21.3 GHz
6P 1/2
F=0
378 nm ABSORPTION
378 nm EMISSION
535 nm EMISSION

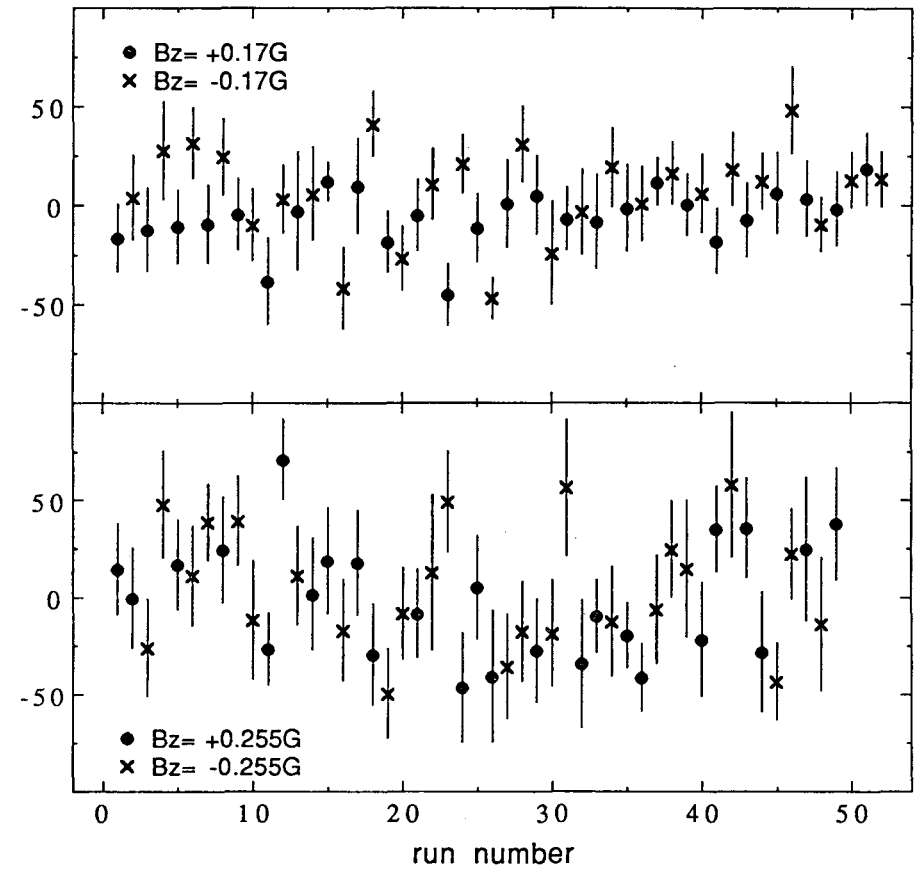
Bz= +0.17G
Bz= -0.17G
50
0
-50
50
0
-50
Bz= +0.255G
Bz= -0.255G
0
10
20
30
40
50
run number

LAWRENCE BERKELEY LABORATORY
UNIVERSITY OF CALIFORNIA
INFORMATION RESOURCES DEPARTMENT
BERKELEY, CALIFORNIA 94720